ν(C≡N) band (Figure 2, inset). We believe the "jump" in absorbance is due to the deposition of Rh-B polymers from the preparative solution onto the fiber itself demonstrating the existence of "in situ" coating of the optical fiber.

Preliminary experiments have shown that these thin films coated on optical fibers adsorb water molecules when exposed to air. The polymers themselves have been shown to be hygroscopic.[12f] Other small molecules of interest may also be adsorbed by these films, undoubtedly due their network-like nature, and this point is now under investigation. Providing that interesting and relevent adsorbates be found one may envision using these and similar coated fibers as chemical sensors.

Acknowledgment. The authors wish to thank Prof. A. Katzir of the School of Physics and Astronomy of Tel-Aviv University for his helpful discussions. We extend our appreciation to Ms. Carmela Barash for her diligent technical aid and Ms. Lily Forte for typing this manuscript. Partial funding for this project was provided by the NCRD (Israel).

Registry No. ($[Rh(CO)_2Cl]_2$)($OCN(C_6H_4$-p-$)_2NCO$) (copolymer), 135366-75-5.

Supplementary Material Available: Relevent experimental and measurement procedures including two diagrams of experimental systems (4 pages). Ordering information is given on any current masthead page.

Pulsed ENDOR and ESEEM Spectroscopic Evidence for Unusual Nitrogen Coordination to the Novel H_2-Activating Fe-S Center in Hydrogenase

Hans Thomann,*[†,‡] Marcelino Bernardo,[†] and Michael W. W. Adams[§]

Corporate Research Laboratory
Exxon Research and Engineering Company
Annandale, New Jersey 08801
Department of Chemistry
State University of New York
Stony Brook, New York 11794
Department of Biochemistry
University of Georgia
Athens, Georgia 30602

Received September 10, 1990

Hydrogenases catalyze the activation of molecular hydrogen: $H_2 = 2H^+ + 2e^-$. The proposed site for H_2 oxidation and production in the Fe-containing hydrogenases is a novel Fe-S center, termed the hydrogenase or H cluster.[1-4] The H cluster of hydrogenase I from the anaerobic N_2-fixing bacterium, *Clostridium pasteurianum*, studied by a variety of spectroscopic techniques[5] has an unknown structure comprised of at least three, and possibly, six, Fe atoms.[5d]

We have studied the coordination structure of the H cluster using a unique combination of pulsed ENDOR spectroscopy,

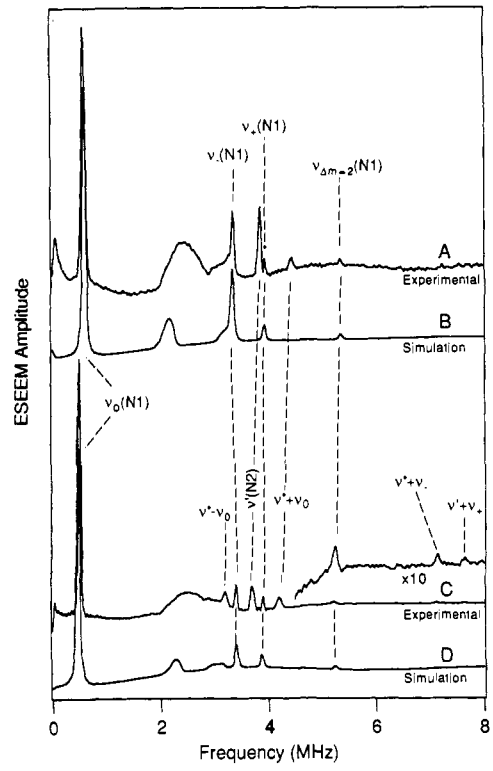

Figure 1. Cosine Fourier transforms of the stimulated electron spin-echo waveforms for experimental data (A and C) and for numerical simulations (B and D). Experimental conditions for A and C: T = 1.7 K; (A) 7.930 GHz, 2706 G, τ = 0.14 μs; (B) 9.087 GHz, 3101 G, τ = 0.18 μs. Simulation parameters for (B and D): e^2qQ/h = 4.85 MHz, η = 0.20, A_{iso} = -1.2 MHz, r_{eff} = 2.8 Å, θ = 90, ϕ = 90, $\alpha = \gamma = 0$, β = 10.

which is the first application of this technique to a metalloenzyme, and electron spin-echo envelope modulation (ESEEM) spectroscopy. The H cluster is coordinated by two nitrogens. One of the two nitrogen atoms has an unusually large quadrupole coupling for a protein nitrogen donor ligand, suggesting a unique coordination structure for the H cluster.

Hydrogenase I was purified and oxidized as previously described.[5a,6] ESEEM and ENDOR data were recorded at several g values and at several microwave excitation frequencies. ESEEM spectra, obtained by cosine Fourier transformation of the three pulse stimulated echo waveforms, recorded at 7.930 and 9.087 GHz, are shown in Figure 1. These spectra were recorded near the extrema, g_{max} = 2.10, of the EPR spectrum[1,5a] to take advantage of the enhanced resolution afforded by g-matrix orientation selectivity.[7,8] The ESEEM frequencies, the frequency shifts between the two microwave excitation frequencies, and the depth of the ESEEM intensities are indicative of covalently coordinated nitrogen.[9]

Quantitative analysis of the ESEEM spectra is possible by tracking the ESEEM frequencies in spectra recorded at multiple microwave excitation frequencies.[10-12] Pure nuclear quadrupole resonance (NQR) transitions can be observed in ESEEM spectroscopy when the local magnetic field vanishes in one of the electron spin manifolds. This occurs when the nuclear Zeeman field is cancelled by the hyperfine field.[10] The three ESEEM transitions in this manifold are pure ^{14}N NQR transitions: ν_0,

[†] Exxon Research and Engineering Company.
[‡] State University of New York.
[§] University of Georgia.

(1) Erbes, D. L.; Burris, R. H.; Orme-Johnson, W. H. *Proc. Natl. Acad. Sci. U.S.A.* **1975**, *72*, 4795-4799.
(2) Chen, J.-S.; Mortenson, L. E.; Palmer, G. In *Iron and Copper Proteins*; Yasunobu, K. T., Mower, H. F.; Hayaishi, O., Eds.; Plenum Publishing Corp.: New York, 1976; pp 68-82.
(3) Hagen, W. R.; van Berkel-Arts, A.; Kruse-Wolters, K. M.; Dunham, W. R.; Veeger, C. *FEBS Lett.* **1986**, *201*, 158-162.
(4) van Dijk, C.; Grande, H. J.; Mayhew, S. G.; Veeger, C. *Eur. J. Biochem.* **1980**, *107*, 251-261.
(5) (a) Adams, M. W. W. *J. Biol. Chem.* **1987**, *262*, 15054-15061. (b) Zambrano, I. C.; Kowal, A. T.; Adams, M. W. W.; Mortenson, L. E.; Johnson, M. K. *J. Biol. Chem.* **1989**, *264*, 20974-20983. (c) Macor, K. A.; Czernuszewicz, R. S.; Adams, M. W. W.; Spiro, T. G. *J. Biol. Chem.* **1987**, *262*, 9945-9947. (d) Adams, M. W. W.; Eccleston, E.; Howard, J. B. *Proc. Natl. Acad. Sci. U.S.A.* **1989**, *86*, 4932-4936.
(6) Protein activity was 810 μmol of H_2 evolved/(min·mg), based on the Lowry method of protein determination. See ref 5d.
(7) Hurst, G. C.; Henderson, T. A.; Kreilick, R. W. *J. Am. Chem. Soc.* **1985**, *107*, 7294-7299.
(8) Reijerse, E. J.; van Earle, N. A. J. M.; Keijzers, C. P. *J. Magn. Reson.* **1986**, *67*, 114-124.
(9) Mims, W. B.; Peisach, J. In *Advanced EPR Techniques, Applications in Biology and Biochemistry*; Hoff, A., Ed.; Elsevier, Amsterdam, 1989.
(10) Mims, W. B.; Peisach, J. *J. Chem. Phys.* **1978**, *69*, 4921-4930.
(11) Reijerse, E. J.; Keijzers, C. P. *J. Magn. Reson.* **1987**, *71*, 83-96.
(12) Flanagan, H. L.; Singel, D. J. *J. Chem. Phys.* **1987**, *87*, 5606-5611.

0002-7863/91/1513-7044$02.50/0

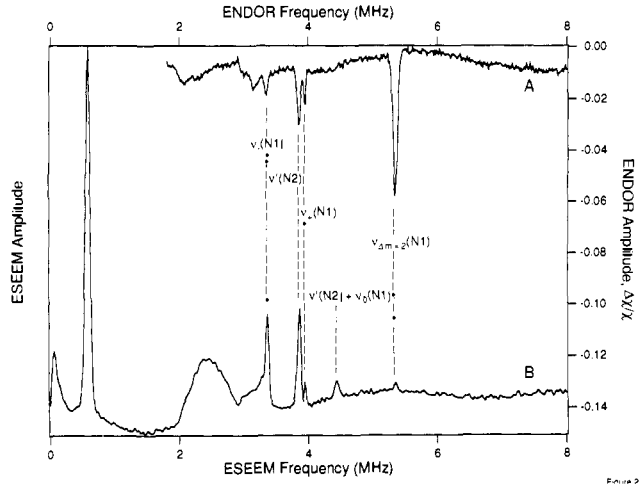

Figure 2. (A) Stimulated echo ENDOR spectrum. Experimental conditions: 9.076 GHz; 3104 G; microwave pulse width 0.05 μs; rf pulse width 65.0 μsec; rf pulse power 100 W; T = 1.61 K. (B) Cosine Fourier transform of the stimulated electron spin echo waveform. Experimental conditions: T = 1.7 K; 9.087 GHz; 3101 G; τ = 0.15 μs.

ν_-, ν_+ from which the quadrupole coupling parameters can be directly calculated.[13] At exact cancellation, the ν_+ transition frequency reaches its minimum value. Near cancellation, the value of the quadrupole coupling deduced from the ESEEM spectrum will be accurate to within 10% for $\nu_n - |A|/2 < 0.25\nu_n$, where $\nu_n = g_n\beta_n B_0/h$.[11]

On the basis of these considerations, the three lines at 0.50, 3.39, and 3.89 MHz recorded at 2706 G (Figure 1A) which shift to 0.58, 3.37, and 3.95 MHz at 3101 G (Figure 1C) are assigned to the ν_0, ν_-, ν_+ NQR transitions for a ^{14}N nucleus, N1. Taking 2706 G as the approximate field for cancellation, the nitrogen quadrupole parameters are K = 1.21 MHz, η = 0.21.[13] The peaks at 2.4 and 5.4 MHz (Figure 1A) arise from transitions in the second electron spin manifold in which the hyperfine field adds to the Zeeman field. The broader 2.4-MHz peak is assigned to the overlapping (ν_0, ν_-) transitions.[14] The 5.23-MHz peak, which shifts to 5.36 MHz at 3101 G, is assigned to the ν_+ or "ΔM_I = 2" transition from this second spin manifold.[15]

The line at 3.68 MHz, ν'(N2) in Figure 1A, shifts to 3.87 MHz in Figure 1C. This is a shift of 0.44 kHz/G, which is close to the gyromagnetic value for the nitrogen nucleus (0.31 kHz/G). ν'(N2) is therefore assigned to a second nitrogen, N2, for which $\nu_n - |A|/2 \gg 0.25\nu_n$ so that pure NQR transitions cannot be observed.[16] The additional lines in Figure 1A, at 3.18 and 4.18 MHz are sum and difference ($\nu' \pm \nu_0$) combination peaks between N1 and N2.[17] Sum peaks between ν'(N2) and the ν_-, ν_+ lines from N1 can also be observed at 7.1 and 7.6 MHz, respectively. At 3101 G, ν' shifts to 3.87 MHz so that, as expected, the $\nu' + \nu_0$ peaks shift to 4.45 and 3.29 MHz, respectively.

The ESEEM line assignments for N1 were further confirmed by numerical simulations[20] in which g-matrix orientation selectivity[21] is explicity incorporated.[18,19] Using the quadrupole parameters obtained directly from the experimental spectrum, the simulated spectra (Figure 1, B and D) quantitatively reproduce both the ESEEM frequencies and intensities and the correct shift of the ESEEM frequencies with shift in microwave excitation frequency. The simulations also establish the orientation of the quadrupole tensor with respect to the g matrix[22] and provide a measure of the hyperfine anisotropy.[23] The isotropic hyperfine coupling, $|A_{iso}|$ = 1.2 MHz, establishes the covalent nature of the nitrogen coupling.

A direct comparison of the ESEEM and ENDOR spectra is shown in Figure 2. Nitrogen ENDOR lines in hydrogenase I are not observed by conventional ENDOR spectroscopy.[24] However, nitrogen ENDOR lines from both N1 and N2 are observed (Figure 2) with use of the stimulated echo ENDOR technique.[25] The combined ESEEM and pulsed ENDOR spectroscopies illustrate the complementary nature of the two techniques[7] and provide a method of corroborating the spectral line assignments. Observation of ESEEM lines requires the coherent excitation of allowed and semiforbidden EPR transitions while ENDOR requires only the excitation of allowed EPR (and NMR) transitions. This has the consequence (given other conditions equal) that ESEEM lines are more intense at lower frequencies while ENDOR lines are more intense at higher frequencies. Combination frequencies between N1 and N2 observed in the ESEEM spectrum are also not expected in the ENDOR spectrum, as confirmed in Figure 2.

The magnitude of the quadrupole coupling, K = 1.21 MHz (e^2qQ/h = 4.85 MHz), for N1 is much larger than previously reported[9,26-29] values for nitrogen atoms in protein residues. It is expected that $e^2qQ/h < 3.4$ MHz, with the largest value arising from peptide nitrogens.[26-30] The quadrupole coupling is determined by the electric field gradient (EFG) on the ^{14}N nucleus, which is in turn determined by the geometry and electronegativity of bonded atoms, thereby imparting a chemical specificity analogous to the chemical shift in NMR.[31] The direct bonding of a nitrogen atom to an iron cation of the positively charged H cluster is expected to decrease, rather than increase, the magnitude of the quadrupole coupling compared to that of a nonbonded nitrogen.[28] This would suggest that N1 is not directly bonded to an iron atom of the H cluster. However, the finite isotropic hyperfine coupling unambiguously establishes a covalent interaction between N1 and the H cluster. Isotropic couplings of similar magnitude have been attributed to peptide nitrogen bonded to FeS centers.[30,32] However, in those cases the quadrupole

(13) The ^{14}N quadrupole coupling constants are related to the ESEEM transitions, ν_0, ν_-, ν_+: $\nu_+ = K(3 + \eta)$, $\nu_- = K(3 - \eta)$, $\nu_0 = 2K\eta$; where $e^2qQ/h = 4K$. See ref 31.

(14) ESEEM lines due to the inner transitions (ν_0, ν_-) from this manifold are usually broadened beyond detectability (due to the contributions from the hyperfine anisotropy) if complete spherical averaging over the orientationally disordered samples is operative.[10,17,18] In the present case, however, these transitions are observed because of g-matrix orientation selectivity.

(15) In the absence of hyperfine anisotropy, the ν_+ or "ΔM_I = 2" transition from the second spin manifold is expected at $2[(\nu_n + A_{iso}/2)^2 + K^2(3 + \eta^2)]^{1/2}$.[11] The difference between the calculated frequencies, 5.4 and 5.7 MHz, and the observed values, 5.25 and 5.36 MHz, at 2706 and 3101 G, respectively, is due to hyperfine anisotropy.

(16) The frequency shifts observed with magnetic field shift at constant g value for the N2 lines indicates that $K \gg \nu_N$ and that $|A|/2 < \nu_N$.

(17) (a) Mims, W. B. *Phys. Rev.* **1972**, *B5*, 2409–2419. (b) McCracken, J.; Pember, S.; Benkovic, S. J.; Villafranca, J. J.; Miller, R. J.; Peisach, J. *J. Am. Chem. Soc.* **1988**, *110*, 1069–1074.

(18) Cornelius, J. B.; McCracken, J.; Clarkson, R. B.; Belford, R. L.; Peisach, J. Preprint.

(19) Jin, H.-Y.; Thomann, H. To be published. Jin, H.-Y. Ph.D. Thesis, 1989, City University of New York.

(20) Simulations were based on the spin Hamiltonian: $\mathbf{H}_s = \beta_e\mathbf{S}\cdot\mathbf{g}\cdot\mathbf{B} + \mathbf{S}\cdot\mathbf{A}\cdot\mathbf{I} - g_N\beta_n\mathbf{B}\cdot\mathbf{I} + K[(3I'^2_z - I^2) + \eta(I'^2_x - I'^2_y)]$, in which the g anisotropy is explicitly incorporated. The hyperfine matrix is represented by an isotropic plus point dipole coupling model. See ref 17 and 18.

(21) Hurst, G. C.; Henderson, T. A.; Kreilick, R. W. *J. Am. Chem. Soc.* **1985**, *107*, 7294–7299.

(22) The relative intensities of the ESEEM lines are predominantly determined by orientation selective excitation and the relative orientations of the principal axis between the g matrix and the nitrogen quadrupole tensor. This accounts for the weak intensity of the "ΔM_I = 2" transition at 5.4 MHz in Figures 1 and 2B.

(23) The hyperfine anisotropy is evident from the frequency shift of the "ΔM_I = 2" transition in ESEEM spectra recorded as a function of the effective g value.

(24) Telser, J.; Benecky, M. J.; Adams, M. W. W.; Mortenson, L. E.; Hoffman, B. M. *J. Biol. Chem.* **1987**, *262*, 6589–6594.

(25) Mims, W. B. *Proc. Roy. Soc.* **1965**, *A283*, 452–457.

(26) Edmonds, D. T. *Phys. Rep.* **1977**, *29*, 233–290.

(27) Ashby, C. H.; Cheng, C. P.; Brown, T. L. *J. Am. Chem. Soc.* **1978**, *100*, 6057–6063.

(28) Ashby, C. I. H.; Paton, W. F.; Brown, T. L. *J. Am. Chem. Soc.* **1980**, *102*, 2990–2998.

(29) Peisach, J.; Mims, W. B.; Davis, J. L. *J. Biol. Chem.* **1979**, *254*, 12379–12389.

(30) Cammack, R.; Chapman, A.; McCracken, J.; Cornelius, J. B.; Peisach, J.; Weiner, J. H. *Biochim. Biophys. Acta* **1988**, *956*, 307–312.

(31) Lucken, E. A. C. *Nuclear Quadrupole Coupling Constants*; Academic Press: London, 1969.

(32) LoBrutto, R.; Haley, P. E.; Yu, C.-A.; Ohnishi, T.; Leigh, J. S. *Biophys. J.* **1986**, *46*, 327a.

coupling was that expected for a peptide nitrogen. We speculate that the unusual coordination which imparts the large quadrupole coupling to N1 is associated with a unique coordination structure which is intimately associated with the catalytic function of the H cluster.

Acknowledgment. The expert assistance of K. E. Stokely in the enzyme preparation is acknowledged and gratefully appreciated. We are grateful to J. Cornelius for making an ESEEM simulation program available to us. The portion of this work performed at the University of Georgia was supported by a grant to M.W.W.A. from the National Science Foundation (Grant DMB-8805255).

Unique Ultraviolet-Visible and Circular Dichroism Behavior Due to Exciton Coupling in a Biscyanine Dye

Dario Gargiulo,[†] Fadila Derguini,[†] Nikolina Berova,[†,‡] Koji Nakanishi,*[,†] and Nobuyuki Harada*[,§]

Department of Chemistry
Columbia University, New York, New York 10027
Institute of Organic Chemistry
Bulgarian Academy of Sciences
BG-1113 Sofia, Bulgaria
Institute for Chemical Reaction Science
Tohoku University, 2-1-1 Katahira
Aoba, Sendai 980, Japan
Received May 31, 1991

The cyanine dyes are characterized by intense and sharp absorption bands in the UV-vis region, and this could provide a powerful new tool for CD studies of biopolymer conformations in solution. The biscyanine dye **3**, prepared during an exploratory search for such chromophores, shows two *distinct and widely separated* vis bands at 550 (ϵ 182000)/480 nm (191000). Moreover, the sign of its exciton-coupled CD curve is negative, i.e., *opposite* to that expected;[1] the bis-Schiff base **4** also exhibits similar properties. In the following we account for this unique behavior.

Reaction of (1*S*,2*S*)-(+)-*trans*-1,2-cyclohexanediamine (**1**) and 7-piperidinohepta-2,4,6-trienal (**2**, merocyanine)[2] followed by flash chromatography yielded biscation **3a**;[3] the reaction was performed in milligram scale, under argon in the dark.[4] Deprotonation of **3a** to bis-Schiff base **4**[3] was achieved in a UV cell; subsequent titration of a solution of **4** by addition of TFA led to spectral changes shown in Figure 1. Neutral **4**, UV-vis, λ_{max} 383 nm (ϵ, 80000), exhibits a bisignate CD, 412 nm ($\Delta\epsilon$ -73), 362 (+63), the Cotton effects (CE's) of which are *opposite* in sign to its dibenzamide **5**[5] and bis-*p*-methoxycinnamate **6**[6] (MeCN), 312 nm ($\Delta\epsilon$ +36), 274 (-25); λ_{max} (MeCN), 287 nm (ϵ 41000). Upon titration of Schiff base **4** with TFA, a new UV-vis peak (Figure 1A) and a negative CD band appeared at 520 nm. The data

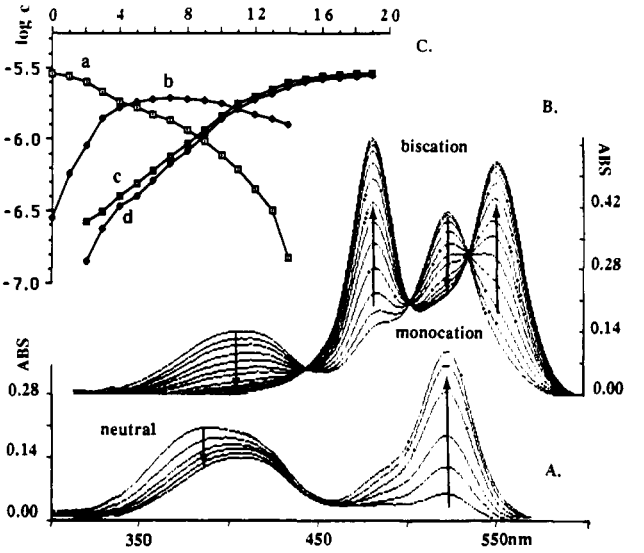

Figure 1. Changes in UV-vis spectrum accompanying stepwise addition of a 5.0×10^{-4} M solution of TFA to a solution of bis-Schiff base **4**, $c = 3 \times 10^{-6}$ M both in CH_2Cl_2. Arrows denote the direction of changes. (A) Equilibrium between neutral Schiff base **4** and monocation. (B) Equilibrium between neutral Schiff base **4**, monocation, and biscation **3b**. (C) Stepwise addition of 20 aliquots of TFA to a solution of neutral Schiff base **4**, both in CH_2Cl_2. Horizontal axis: Each aliquot represents 1.56×10^{-3} μmol of TFA (5.0×10^{-4} M solution) added to 1.3 mL of a 3.00×10^{-6} M solution of **4**. Vertical axis: log molar concentration of respective species, calculated from ϵ values. (a) Neutral, 383 nm (ϵ 80000); (b) monocation, 522 nm (207000); (c) biscation, 480 nm (191000); (d) biscation, 550 nm (192000).

Scheme I

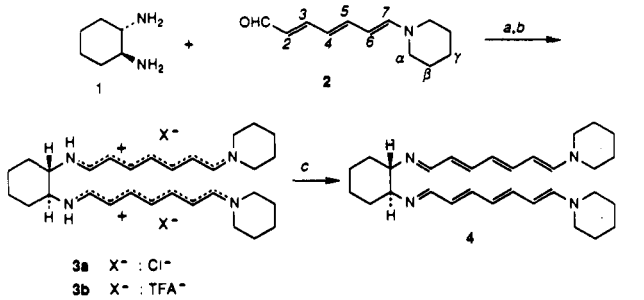

[a] (a) Dry MeOH, 60-65 °C, 4 h. (b) SiO_2 flash chromatography, MeOH/$CHCl_3$/1 N HCl (20/80/0.4). (c) CH_2Cl_2/NaOH.

indicate the formation of the monocation species, λ_{max} 522 nm (cf., the monocyanine from cyclohexylamine, λ_{max} 515 nm, CH_2Cl_2). Under more acidic conditions, the monocation peak is displaced by *two* strong UV-vis maxima at 550/480 nm (Figure 1B) accompanied by intense bisignate CE's with signs opposite to that expected (Figure 2).

Two mechanisms are conceivable for the appearance of two vis peaks: coexistence of two species absorbing at different wavelengths, or exciton coupling in biscation **3b**. The first possibility can be discounted because the titration curves plotted at 550 and 480 nm are very similar, indicating the presence of a single species (Figure 1C, curves c and d). The following aspects support an exciton coupling mechanism: (i) the two peaks at 550 and 480 nm are equidistant from that of the monocyanine (515 nm); and (ii) the CD shows bisignate CE's of similar intensities. Such large separations of the two UV-vis peaks arising from exciton coupling have only been encountered in anthracene crystals[7] and not in solution.[8]

The biscyanine dye **7** (structure in Figure 2) was chosen as the model to calculate the preferred conformation by MMP1 and

[†] Columbia University.
[‡] On leave from the Bulgarian Academy of Sciences.
[§] Tohoku University.

(1) Harada, N.; Nakanishi, K. *Circular Dichroic Spectroscopy—Exciton Coupling in Organic Stereochemistry*; University Science Books: Mill Valley, CA; and Oxford University Press: Oxford, 1983.

(2) Prepared according to: Derguini, F.; Caldwell, C. G.; Motto, M. G.; Balogh-Nair, V.; Nakanishi, K. *J. Am. Chem. Soc.* **1983**, *105*, 646. UV (CH_2Cl_2) 422 nm (ϵ 56000); ^{1}H NMR (CD_3OD) δ 1.70 (m, 6 H, β,β',γ-CH_2), 3.30 (m, α,α'-CH_2, masked by solvent), 5.48 (t, J = 12.5 Hz, 6 H), 5.80 (dd, J = 14, 9 Hz, 2 H), 6.07 (dd, J = 14, 12.5 Hz, 4 H), 6.85 (d, J = 12.5 Hz, 7 H), 6.92 (dd, J = 14, 12.5 Hz, 5 H), 7.30 (dd, J = 14, 12.5 Hz, 3 H), 9.17 (d, J = 9 Hz, 1 H).

(3) **3a**: FTIR ($CHCl_3$/MeOH) 2400, 1529, 1389, 1211 cm^{-1}; MS (FAB/glycerol), **3a** deprotonates in the matrix leading to the $M+1$ peak for **4** at 461; the NMR could not be measured due to instability under our sample preparation conditions. **4**: FTIR ($CHCl_3$/MeOH) 1477, 1371, 1195 cm^{-1}.

(4) Malhotra, S. S.; Whiting, M. C. *J. Chem. Soc.* **1960**, 3812.

(5) Kawai, M.; Nagai, U.; Katsumi, M. *Tetrahedron Lett.* **1975**, 3165.

(6) Prepared according to: Wiesler, W. T.; Berova, N.; Ojika, M.; Meyers, H. V.; Chang, M.; Zhou, P.; Lo, L. C.; Niwa, M.; Takeda, R.; Nakanishi, K. *Helv. Chim. Acta* **1990**, *73*, 509.

(7) Craig, D. P.; Hobbins, P. C. *J. Chem. Soc.* **1955**, 539.

(8) Some bis-naphthalenoids show ca. 15 nm separation: Imajo, S.; Kato, A.; Shingu, K.; Kuritani, H. *Tetrahedron Lett.* **1981**, 2179.

0002-7863/91/1513-7046$02.50/0